

Prolonging assembly through dissociation: A self-assembly paradigm in microtubules

Sumedha, Michael F. Hagan, and Bulbul Chakraborty

Martin Fisher School of Physics, Brandeis University, Waltham, Massachusetts 02454, USA

(Received 19 August 2009; revised manuscript received 29 March 2011; published 3 May 2011)

We study a one-dimensional model of microtubule assembly and disassembly in which GTP bound to tubulins within the microtubule undergoes stochastic hydrolysis. In contrast to models that consider only a cap of GTP-bound tubulin, stochastic hydrolysis allows GTP-bound tubulin remnants to exist within the microtubule. We find that these buried GTP remnants enable an alternative mechanism of recovery from shrinkage and enhances fluctuations of filament lengths. Under conditions for which this alternative mechanism dominates, an increasing depolymerization rate leads to a decrease in dissociation rate and thus a net increase in assembly.

DOI: [10.1103/PhysRevE.83.051904](https://doi.org/10.1103/PhysRevE.83.051904)

PACS number(s): 87.10.-e, 02.50.Ey, 05.40.-a, 87.17.Aa

Microtubules are semiflexible polymers that serve as structural components inside the eukaryotic cell and are involved in many cellular processes such as mitosis, cytokinesis, and vesicular transport [1–3]. In order to perform these functions, microtubules (MTs) continually rearrange through a process known as dynamic instability (DI), in which they switch from a phase of slow elongation to rapid shortening (catastrophe), and from rapid shortening to growth (rescue) [1]. The basic self-assembly mechanism underlying DI, assembly mediated by nucleotide phosphate activity, is omnipresent in biological systems. In this paper we study a minimal nonequilibrium model of DI that shows enhanced assembly with increasing depolymerization rate. This provides a new paradigm of self-assembly, which can occur only in nonequilibrium systems, and in the context of DI could explain some puzzling results about the influence of proteins on MT assembly [4].

With recent advances in experimental techniques [5–7], it has become possible to quantify MT dynamics at a nanoscale and, thereby, provide more stringent tests of models. Models such as ours can provide insight into the nonequilibrium phenomena of self-assembly and provide a palette of scenarios. While it is established that GTP hydrolysis is essential to DI, the mechanisms that underlie DI are not fully understood. In this paper we study a minimal model of DI that involves stochastic (or random) hydrolysis (SH), a mechanism that has received relatively little attention compared to interfacial (or vectorial) hydrolysis (IH) that forms the basis of cap models [8,9]. We study a particular SH model [10,11], which in contrast to a SH model that takes into account all thirteen protofilaments of a MT [12], depicts the MT as a $1-d$ sequence with rates that prescribe polymerization, depolymerization, and hydrolysis. The focus of our work is to relate the functioning of MT's to GTP remnants that are characteristic of SH models.

MTs are formed by assembly of $\alpha - \beta$ tubulin dimers, which are polar and impart polarity to MTs. MTs grow mainly from the end that has exposed β tubulin and are composed of (typically) 13 linear protofilaments [1]. While a free tubulin dimer has a GTP molecule bound to each monomer, incorporation into a MT activates the β -tubulin monomer for hydrolysis of its associated GTP. GDP-bound tubulin is less stable within the MT lattice [13], and hence a GDP-bound tubulin at the tip of a MT has a higher rate of detachment (depolymerization) than a GTP-bound tubulin. GTP hydrolysis is essential to DI. Models in the IH class

assume that all hydrolysis occurs at a sharp interface between GDP-bound and GTP-bound tubulins [8,9], whereas in SH-based models, hydrolysis occurs stochastically, anywhere in the MT [10–12,14–16].

In contrast to IH models, SH models lead to GTP monomers being located throughout the MT, with a concentration that decays exponentially with distance from the growing end [11]. These models allow for a repolymerization mechanism that involves these GTP remnants; i.e., as the MT depolymerizes by detachment of GDP tubulins, the remnants get exposed and the MT starts polymerizing again. Support for the presence of GTP tubulins inside the MT has been provided by recent experiments [5]. The remnant-mediated repolymerization leads to the possibility of extending activity through increased depolymerization rates.

Our model [10,11] represents the MT by a linear sequence of two species of monomers, which correspond to GTP-bound tubulin (denoted by $+$ in this paper) and GDP-bound tubulin (denoted by $-$). We assume that the MT undergoes attachment and detachment only at one end, which we call the growing end (sometimes called the $+$ end in the literature). A MT evolves via the following rules (illustrated in Fig. 1):

(1) *Attachment*: If the growing tip is a $+$ monomer, it grows with rate λ by addition of a $+$ subunit.

(2) *Detachment*: A $-$ monomer at the growing end detaches with rate μ , causing its shrinkage.

(3) *Hydrolysis*: With rate 1 any $+$ monomer in the MT can undergo hydrolysis to yield a $-$ monomer.

(4) *Attachment*: $+$ subunits could attach to a growing end with a $-$ monomer at the tip with rate $p\lambda$ ($p \leq 1$).

A previous study of the model [11] for $p > 0$, demonstrated a transition from a phase of bounded to unbounded growth of the MTs. The present study focuses on low p and fluctuations in the bounded growth region of the phase diagram. The effect of remnants on dynamics of MTs is strongest for the $p = 0$ model, which we call the *GTP remnants model* since the only mode of recovering from depolymerization is via remnants. Recent experiments indicate correlation between the presence of remnants with events where the MT switches from shrinkage to growth. In particular, Perez *et al.* [5] observe GTP-bound tubulin within MTs and find that the location of these remnants correlates to locations at which such events occurred during MT growth.

In the remnants model, if the number of GTP monomers fluctuates to 0, growth is no longer possible and the MT

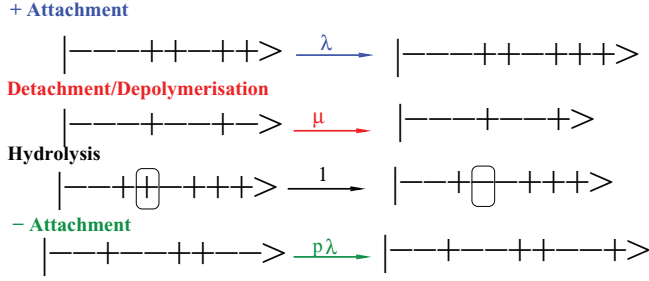


FIG. 1. (Color online) Schematic of microtubule dynamics. We assume that all the activity occurs at the right end (denoted by >) of the MT.

undergoes a complete catastrophe with no possibility of rescue. Any process that exposes remnants promotes growth fluctuations and makes the MT remain active for longer. In particular, increasing μ at fixed λ leads to longer times (t_N), and higher maximum lengths ($L(t_N)$) of MTs before complete loss of GTP. Beyond t_N , the MT undergoes a catastrophe and shrinks to zero in time of order of $L(t_N)/\mu$. During the time t_N , the MT remains active and in an overall growth phase with shrinkage and growth fluctuations resulting from depolymerization and remnant-mediated polymerization events. The shrinkages occurring during the active phase have a qualitatively different character from the catastrophe that occurs after time t_N .

Figure 2 shows numerical results $\langle t_N \rangle$ as a function of μ for a range of values of λ . It is clear that the activity time increases monotonically with increasing λ and μ . For a given λ , $\langle t_N \rangle$ increases with increasing μ and eventually saturates at a value of the order of $\exp(\lambda)/\lambda$. In Fig. 2 we also show numerically obtained values of the average growth velocity ($v = \langle L(t_N) \rangle / \langle t_N \rangle$) at time t_N . The velocity increases with increasing λ and μ , and for a given λ , it saturates for large μ . As illustrated in Fig. 2, $v = (\lambda - 1)\mu / (1 + \mu)$ leads to good scaling collapse of the data. Both of these features illustrate the increase in activity with increasing *depolymerization* rate, which is a hallmark of growth fluctuations initiated by the presence of remnants. As

shown below, $-$ attachment events do not destroy this signature for small p . In order to get a better understanding of the effect of μ on the dynamics during the growth phase, we analyze the equations for the probability distribution of the lengths at $\mu = 0$ where we have only polymerization and hydrolysis. The probability distribution of total length $L(t)$ of the MT at time t obeys the equation

$$\frac{dP(L,t)}{dt} = \lambda(1 - n_0(t))[P(L-1,t) - P(L,t)] + \mu n_0(t)[P(L+1,t) - P(L,t)], \quad (1)$$

where $n_0(t)$ is the probability of having a GDP at the tip of MT and is given by

$$\frac{dn_0(t)}{dt} = 1 - n_0(t) - \mu n_0(t)P(+ - >, t). \quad (2)$$

Here $P(+ - >, t)$ is the conditional probability that, given the tip of the MT is a $-$, the second last tubulin dimer is a $+$. A configuration with $|+ - >$ at the tip can be reached either by depolymerization of $|+ - - >$ state or by hydrolysis of a $|+ + >$ state. The probability of having a $|+ - - >$ configuration further depends on $|+ - - - >$, leading to a hierarchy of equations that cannot be solved exactly. It is, therefore, not possible to obtain an exact expression for $P(L,t)$ for arbitrary values of λ and μ .

For $\mu = 0$, and arbitrary λ , Eq. (2) does not couple $n_0(t)$ and $P(+ - >, t)$, and we obtain the solution: $n_0(t) = 1 - \exp(-t)$. Substituting in Eq. (1) leads to

$$P(L,t) = e^{[-\lambda(1-e^{-t})]} \frac{[\lambda(1-e^{-t})]^L}{L!}. \quad (3)$$

The average length at any time $\langle L(t) \rangle = \lambda(1 - \exp(-t))$. Similarly, the average number of GTP-bound tubulins at time t is $\langle T(t) \rangle = \lambda t \exp(-t)$. There is, therefore, a characteristic time at which the amount of GTP goes to zero (purely through hydrolysis), and this time $\langle t_N \rangle$ scales roughly as $\ln(\lambda)$. Beyond this time, the MT becomes completely inactive since for $p = 0$ and $\mu = 0$, the first and third processes illustrated in Fig. 1 cannot occur.

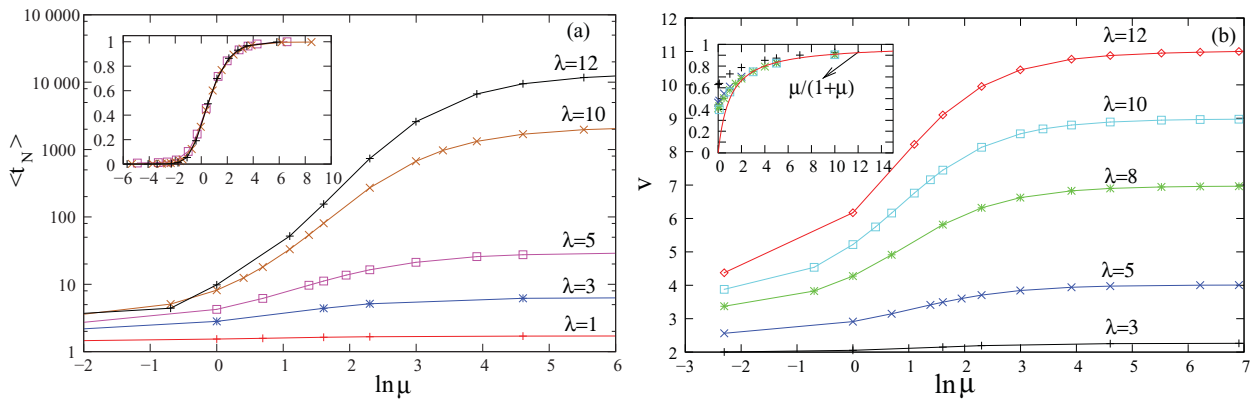


FIG. 2. (Color online) (a) The average time at which the number of GTP-bound subunits goes to zero ($\langle t_N \rangle$) as a function of $\ln \mu$. The inset shows a scaling collapse of the plots, with y axis scaled by e^λ / λ and the x axis displaced by λ , for $\lambda = 8, 10, 12$. (b) The average growth velocity ($v = \langle L(t_N) \rangle / \langle t_N \rangle$) for indicated values of λ as a function of $\ln \mu$. In the inset we have scaled v for $\lambda = 3, 5, 8, 10, 12$, and $\mu > 1$, by $(\lambda - 1)$ to illustrate the scaling collapse implied by Eq. (6) for different values of λ . We find the scaled values lie on the $\mu / (1 + \mu)$ curve. The scaling holds for $\lambda \geq 8$, with data for $\lambda = 5$, showing deviations at small values of μ .

Introducing a nonzero μ enables depolymerization, which dramatically changes assembly behavior by exposing remnants buried inside the MT to offer the possibility of growth fluctuations. Numerical results demonstrate an exponential dependence of t_N on λ for large μ (indicated by the scaling collapse in Fig. 2). As seen in Fig. 2, $\langle t_N \rangle$ increases monotonically from a value of order $O(\ln \lambda)$ to a value of order $\exp(\lambda)$ as we increase μ from 0 to ∞ . The distributions of t_N and $L(t_N)$ for various λ and μ (Fig. 4) broaden with increasing μ , reaching asymptotic forms for $\mu \gg \lambda$. The increase of fluctuations, indicated by these broadening distributions, is a consequence of the remnants.

It is difficult to obtain analytic solutions to Eq. (2) at finite values of μ because of the coupling between n_0 and $P(+ - >, t)$. In the limit of $\lambda \rightarrow \infty$, $\mu \rightarrow \infty$, the problem becomes simple again because $P(+ - >, t) \simeq 1$ for all t since hydrolysis is a rare event. For arbitrary values of μ and λ , the dynamics at times $t \ll t_N$ is also dominated by attachment and detachment events, and hydrolysis is not effective at converting GTP to GDP between attachment and detachment events. It, therefore, seems plausible that the dynamics during the active (growth) phase of the MT can be approximately described by assuming $P(+ - >, t) = 1$. An indirect estimate of $P(+ - >, t)$ can be obtained by analyzing the statistics of the size of disassembly events since $P(+ - >, t)$ should be proportional to probability of disassembly events of size 1. For finite values of λ and μ , we found numerically that most disassembly events in the active phase ($t \ll t_N$) involved $O(1)$ sites. Figure 3 shows $P(s)$, the distribution of the size of all the disassembly events except the final complete disassembly for $\lambda = 5$ and $\mu = 1, 2, 5, 10$, and 100, obtained by averaging over 10 000 growth events. In the inset to Fig. 3, we show $P(s, t)$, the average probability of dissociation of size s occurring over a time period t for $\mu = 5$ distributions, are very similar to the $P(s)$ shown in the main plot. Qualitative change in the distribution occurs only if we include the final disassembly event, the complete catastrophe. The distribution, $P(s)$, is exponential for all values of μ , and the average size of a

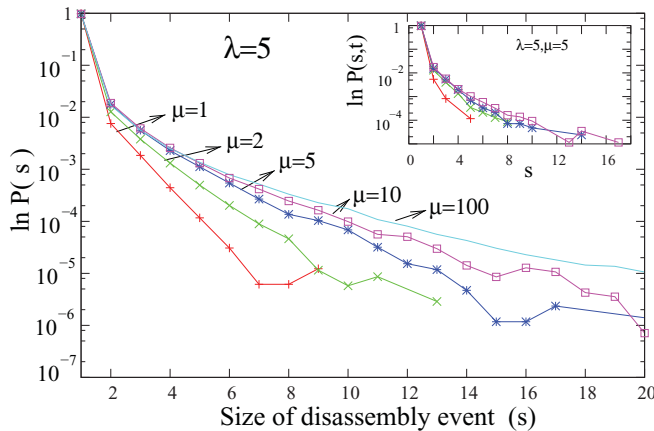


FIG. 3. (Color online) Average probability distribution of size of disassembly events for $\lambda = 5$ on a semilog plot. Average is calculated by looking at all the disassembly events except the final complete disassembly. Inset shows the same distribution for $\lambda = 5$ and $\mu = 5$ when the average is done over time $t = 0.08t_N(+)$, $0.2t_N(\times)$, $0.4t_N(*)$, and $t_N(\square)$.

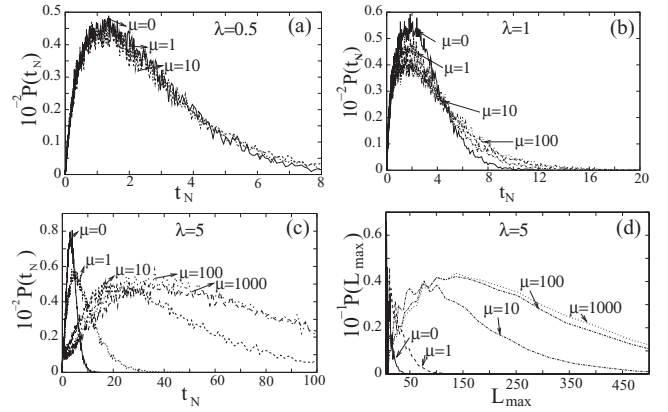


FIG. 4. (a)–(c) The distributions of times at which the amount of GTP in the MT goes to zero (t_N). The distribution shifts to the right with increasing μ until it saturates. (d) The distribution of maximum lengths for $\lambda = 5$. The distributions of maximum lengths and t_N have similar dependencies on μ .

disassembly event varied from 1.013 to 1.06 as μ was changed from 1 to 100.

Our analysis suggests that growth occurs predominantly through a process in which the $-$ at the tip detaches before the hydrolysis of $+$ next to the tip. This picture of the dynamics for $t \ll t_N$ is consistent with our expectation that it is the competition between the tip detachment and the hydrolysis of the $+$ next to the tip that determines the value of t_N . There are, of course, rare events where larger size disassembly events occur during the growth phase, but we expect them not to influence the dynamics of the MT significantly. Hence, we take $P(+ - >, t) \approx 1$ as a good approximation for our model MT in its active (growth) phase. Setting $P(+ - >, t) = 1$, in Eq. (2) we obtain

$$n_0(t) = \frac{1}{1 + \mu} (1 - \exp^{-t(1+\mu)}). \quad (4)$$

Substituting in Eq. (1) leads to

$$P(L, t) = (\lambda)^{L/2} I_L \left(\frac{2\mu t \lambda^{1/2}}{1 + \mu} \right) \exp \left[-\frac{\mu(\lambda + 1)t}{1 + \mu} \right], \quad (5)$$

where $I_L(x)$ is the modified Bessel function of first kind, and Eq. (5) leads to

$$\langle L(t) \rangle = \frac{\mu(\lambda - 1)}{(1 + \mu)} t. \quad (6)$$

Equation (6) implies that the μ dependence of the growth velocity curves for different values of λ can be scaled on to one another, and that the scaled function is $\mu/(1 + \mu)$.

In Fig. 2 (right) we have plotted the numerical results for the velocity for a range of λ and μ values. As shown in the inset, on scaling the average velocity in the growth regime with $(\lambda - 1)$ we get a scaling collapse for different λ , and the scaled function is $\mu/(1 + \mu)$. Strictly speaking, the approximation, $P(+ - >, t) = 1$, which leads to Eq. (6) applies only for times much shorter than t_N . Numerical results, however, indicate that the approximation remains valid even for times pretty close to t_N , and Eq. (5) provides a good description for the dynamics throughout the growing phase. The variance of the distribution

$P(L, t)$ is predicted by Eq. (5) to be $\frac{\mu(\lambda+1)}{1+\mu}t$ and qualitatively describes the numerical results (Fig. 4). One can also solve for the distribution $T(t)$. The average value $\langle T(t) \rangle$ obeys the equation

$$\frac{d \langle T(t) \rangle}{dt} = \lambda[1 - n_0(t)] - \langle T(t) \rangle. \quad (7)$$

Assuming $P(+ \rightarrow, t) = 1$, we get

$$\langle T(t) \rangle = \frac{\lambda\mu}{1+\mu} - \frac{\lambda \exp[-(1+\mu)t]}{\mu(1+\mu)} - \frac{\lambda(\mu-1) \exp(-t)}{\mu}.$$

This equation also matches the simulation results, where we found that the average amount of GTP in the MT during the growing phase fluctuates around $\frac{\lambda\mu}{(1+\mu)}$.

We do not have a good understanding of why assuming $P(+ \rightarrow, t) = 1$ describes the dynamics of our model over a large range of parameters. If we, however, assume that this is a good approximation, then we can make a number of other predictions, which apply to the growing phase, $t \ll \langle t_N \rangle$, and can be subjected to experimental tests. For example, the average number of disassembly events at time t in which the MT switches from a growing to a shrinking phase is given, to leading order by $\langle C(t) \rangle = \frac{\mu^2 t}{(1+\mu)^2}$, and the average number of GTP islands in the MT is predicted to be $\frac{\lambda\mu[1-\exp(-2t)]}{2(1+\mu)}$. All of the predictions presented above reflect the sensitivity of dynamical properties to the depolymerization rate μ and are a fingerprint of remnants. Experimental tests of these predictions can, therefore, provide insight into the nature of hydrolysis and polymerization-depolymerization mechanisms in DI.

Recent experiments [6] monitored the distribution of lengths of growing and shortening excursions within the growth phase in *in vitro* systems of MTs. These experiments were able to resolve fluctuations at the monomer level, and the distributions were found to be exponential. In simulations of our model we find that for small values of p the growth excursions are independent of μ and can be fitted well by $\exp(-\delta l/\lambda)/\lambda$ (δl is the length of the excursion), and the distribution of shortening excursions broadens with μ (Fig. 5). We can fit the experimental data on the distribution of excursions [6] with our model by taking $\lambda = 12$, $\mu \approx 0.1$, $0 < p \leq 0.001$ (Fig. 5).

The main conclusion from fitting the model predictions to experiments is that we need a small value of p to describe the observed growth and shrinkage fluctuations. For $p \simeq 1$, the dynamics of the remnants model becomes qualitatively similar to IH models since remnants do not play a significant role. The small value of p obtained from the fits would then suggest that the presence of remnants is important to understand the statistics of the growth and shrinkage fluctuations. It should be mentioned that in fitting the model predictions to experimental data, we have ignored the shrinkage events involving one site. The rationale is that we believe that experiments cannot resolve these events, which correspond to the loss of one unit in one protofilament. We have not mapped the parameters of our one-dimensional model to that of a 13 protofilament MT, and therefore the actual correspondence between quantitative results of our simulations and experiments is unclear. We can expect to capture trends in behavior with our model. For example, measurement of the

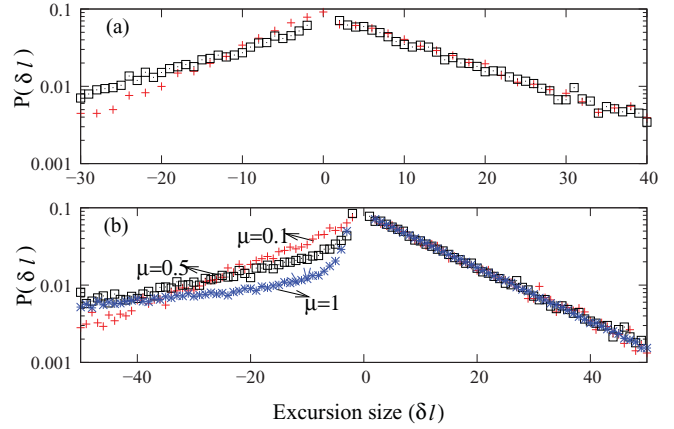


FIG. 5. (Color online) (a) Comparison of excursions (δl) predicted by the GTP remnants model (\square) with $\lambda = 12$, $p = 0$, $\mu = 0.1$, and experimental measurements ($+$) [6] (δl is measured in nm in the experiment). (b) The distribution of excursions with $\lambda = 12$; $p = 0$ for $\mu = 0.1, 0.5$, and 1 . While growth excursions have the distribution $\exp(-\delta l/\lambda)/\lambda$, the distribution of shortening excursions changes from being exponential to nonexponential and broader distributions with increasing μ .

change in shape of the distribution of shortening excursions for experiments performed under different conditions that affect the depolymerization rate could be compared to the shape change predicted by the model (Fig. 5).¹ We have also plotted a typical trajectory with these values of the parameters in the inset of Fig. 6. For these low values of p obtained from the fits, GTP remnants are the dominant source of recovery from negative growth events.

The above analysis was restricted to $p = 0$ in order to highlight the effect of remnants. The rate of $-$ attachments can depend on the environment of the MT, and one can express a crossover from a remnant-dominated dynamic regime to a “cap-dynamics” regime as p is increased. As p is increased, the dynamics changes from cessation of negative growth primarily due to remnants at small p to nonremnant attachment events that are also present in IH models at $p \simeq 1$. Figure 6 shows the time trace for MT length for a representative run for $p = 0$ and 0.01 . Analysis of these trajectories shows that a small, nonzero value of p introduces rare $-$ attachment events (indicated by arrows in the figure). These events change the overall length of MT, but the statistics of positive and negative growth excursions remain similar to $p = 0$. Measurement of these statistics is possible in experiments such as the one analyzed above and should provide tests of the remnant-induced mechanism of growth fluctuations.

Our model can be easily extended to accommodate more detailed features of MTs while keeping the basic mechanism of remnant-induced growth. Parameters can be obtained from simulations by systematically mapping simulations of

¹Note that growth-phase shortening excursions are distinct from rapid shortening, which is more than an order of magnitude faster and typically persists for micrometers rather than nanometers.

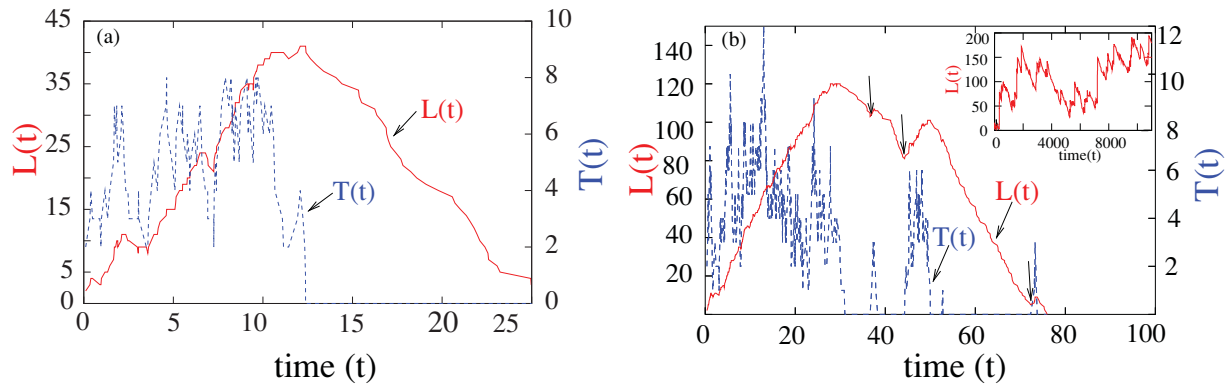


FIG. 6. (Color online) MT length $L(t)$ (solid lines) as a function of time for $\lambda = 5, \mu = 4$, and $p = 0$ (a), $p = 0.01$ (b). The dotted lines show the total amount of GTP $T(t)$ as a function of time for the same runs. Arrows in the second plot indicate the – attachment events due to $p > 0$. The inset shows MT length $L(t)$ for $\lambda = 12, \mu = 0.1$, and $p = 0.0007$. This trajectory looks qualitatively similar to the ones observed experimentally, and these growth-phase fluctuations are different from the rapid shrinkage and slow growth observed in catastrophes and rescues [6].

microscopic models to our effective model. For example, spatially varying hydrolysis rates due to the structure of MTs [12] can be modeled by quenching some GTP-bound sites in our one-dimensional model. Similarly, the effect of motors that mechanically depolymerize MTs without dependence on GTP states [17] can be modeled by assuming a depolymerizing rate μ for both GTP and GDP-bound tubulins.

Preliminary studies of the model with quenched disorder indicate that, although the time for which MT grows changes and there is a transition to unbounded growth as a function of percentage of quenched sites, the distribution of excursions and velocity of growth remains unchanged and therefore is a robust feature of the remnant model. Studies of the model mimicking motors also indicate that the basic features of the remnant model remain unchanged as long as $\lambda > \mu + 1$.

To summarize, we have studied the role of GTP remnants in MT dynamics and shown that remnants give rise to features of DI that are very different from IH models that have no remnants. Some particularly notable features are (1) the average catastrophe time increases with depolymerization rate, (2) the distribution of MT lengths and time of growth depends on λ and μ , broadening as λ and μ are increased, (3) the velocity of growth, besides depending on the free tubulin

concentration (through λ), also depends on depolymerization and hydrolysis rates. Similar behavior was reported by Cassimeris *et al.* [4]. They found that increasing concentration of XMAP resulted in increase of both depolymerization rate and growth velocity. These features are robust, and with recent progress in experimental techniques [5,6] should provide tools for resolving the mechanism of hydrolysis inside a MT. In conclusion, a minimal model of MT dynamics where cessation of negative growth is dominated by GTP remnants leads to a strong spatial structure-dynamics connection. The simplicity of our model allows us to make analytic predictions that can be tested experimentally and to provide sensitive tests for the remnant-mediated mechanisms of growth in MT dynamics, both *in vivo* and *in vitro*. Interestingly, at the same tubulin concentration, MTs exhibit much higher growth rates *in vivo* in comparison to *in vitro* [2,18]. In a broader context, the model illustrates a new paradigm of nonequilibrium self-assembly where assembly is promoted through depolymerization.

We thank the authors of Ref. [6] for providing us with their data for MT excursions *in vitro*. S. and M.F.H. acknowledge support by NIH grant R01AI080791, and S., M.F.H., and B.C. were supported in part by the Brandeis NSF-MRSEC.

-
- [1] E. Karsenti, F. Nedelec, and T. Surrey, *Nat. Cell Biol.* **8**, 1204 (2006).
 [2] A. Desai and T. J. Mitchison, *Annu. Rev. Cell Dev. Biol.* **13**, 83 (1997).
 [3] J. Howard and A. A. Hyman, *Nature (London)* **422**, 753 (2003).
 [4] L. Cassimeris, N. K. Pryer, and E. D. Salman, *J. Cell Biol.* **127**, 985 (1994).
 [5] A. Dimitrov, M. Quesnolt, S. Moutel, I. Cantaloube, C. Pous, and F. Perez, *Science* **322**, 1353 (2008).
 [6] H. T. Schek, M. K. Gardner, J. Cheng, D. J. Odde, and A. J. Hunt, *Curr. Biol.* **17**, 1445 (2007).
 [7] J. Howard and A. A. Hyman, *Nat. Rev. Mol. Cell Biol.* **10**, 569 (2009).
 [8] P. M. Bayley, M. J. Schilstra, and S. R. Martin, *J. Cell Sci.* **95**, 33 (1990); M. Dogterom and S. Leibler, *Phys. Rev. Lett.* **70**, 1347 (1993); H. Flyvbjerg, T. E. Holy, and S. Leibler, *ibid.* **73**, 2372 (1994).
 [9] D. Vavylonis, Q. Yang, and B. O. Shaughnessy, *Proc. Natl. Acad. Sci. U.S.A.* **102**, 8543 (2005); E. B. Stukalin and A. B. Kolomeisky, *Biophys. J.* **90**, 2673 (2006).
 [10] B. Chakraborty and R. Rajesh (unpublished).

- [11] T. Antal, P. L. Krapivsky, S. Redner, M. Mailman, and B. Chakraborty, *Phys. Rev. E* **76**, 041907 (2007); T. Antal, P. L. Krapivsky, and S. Redner, *J. Stat. Mech.* (2007) L05004.
- [12] V. Van Buren, D. J. Odde, and L. Cassimeris, *Proc. Natl. Acad. Sci. U.S.A.* **99**, 6035 (2002); V. van Buren, L. Cassimeris, and D. J. Odde, *Biophys. J.* **89**, 2911 (2005).
- [13] Y. Gebremichael, J. W. Chu, and G. A. Voth, *Biophys. J.* **95**, 2487 (2008).
- [14] T. L. Hill, *Biophys. J.* **49**, 981 (1986).
- [15] H. Flyvbjerg, T. E. Holy, and S. Leibler, *Phys. Rev. E* **54**, 5538 (1996).
- [16] G. Margolin, I. V. Gregoret, H. V. Goodson, and M. S. Alber, *Phys. Rev. E* **74**, 041920 (2006).
- [17] V. Varga, J. Helenius, K. Tanaka, A. A. Hyman, T. U. Tanaka, and J. Howard, *Nat. Cell Biol.* **8**, 957 (2006); K. E. Cullen, *Journal* **83**, 1809 (2002).
- [18] L. Cassimeris, *Cell Motil. Cytoskel.* **26**, 275 (1993).